ISSN 1063-7826, Semiconductors, 2018, Vol. 52, No. 8, pp. 986–992. © Pleiades Publishing, Ltd., 2018.
Original Russian Text © A.G. Rokakh, M.I. Shishkin, V.S. Atkin, 2018, published in Fizika i Tekhnika Poluprovodnikov, 2018, Vol. 52, No. 8, pp. 853–859.

SURFACES, INTERFACES, AND THIN FILMS

On Recombination Processes in CdS–PbS Films

A. G. Rokakh[a], M. I. Shishkin[a]*, and V. S. Atkin[a]

[a] *Saratov State University, Saratov, 410012 Russia*

**e-mail: shishkin1mikhail@gmail.com*

Submitted July 12, 2017; accepted for publication September 5, 2017

Abstract—The transverse and longitudinal photoconductivity, photoluminescence, and cathodoluminescence of sublimated $(CdS)_{0.9}$–$(PbS)_{0.1}$ films at room temperature and upon cooling are studied. The role of inclusions of the narrow-gap phase in the processes is shown. The films are excited over the entire active surface and pointwise (within one crystallite). The surface recombination rate and the lifetime of majority charge carriers at different generation rates and characters of excitation are estimated. A comparative table of recombination parameters of CdS and CdS–PbS films is presented.

DOI: 10.1134/S1063782618080171

1. INTRODUCTION

Polycrystalline heterophase films made from limited CdS–PbS alloys with different fractions of the narrow-gap component possess a high photosensitivity (multiple change in the resistance) and luminescence properties [1, 2] and, in addition, are stable because of resistance to degradation [3]. Since an increase in the fraction of PbS reduces the photosensitivity (multiplicity of the change in the resistance), the optimal relation between the components in the initial mixture corresponds to the CdS(90%)–PbS(10%) composition [4]. Upon activating annealing of the films, their properties are substantially modified, which is favored also by recrystallization and by the simultaneously occurring formation of alloys and their decomposition into individual phases at the film surface and in the bulk. In addition, the films served as a model material for observation and study of the secondary-ion photoeffect (SIPE) [5], the basic effect in emerging optoionics intended to contribute to the technology of nanostructures.

Previous studies [6, 7] aimed at extensive analysis of the characteristics of CdS–PbS films gave interesting results and grounds to continue studying these systems by a set of different methods. For example, the accumulation of crystallites formed from the narrow-gap phase was detected at the film surface, and structural modification of the films upon laser annealing was studied. At the same time, studies of the sample by such measurements is accompanied by the formation of a large number of nonequilibrium charge carriers; however, their influence has not been adequately explored. The purpose of this study is to investigate the specific features of recombination (including radiative recombination) in films on the generation of nonequilibrium charge carriers by different methods (by exposure to coherent and noncoherent light and an electron beam) and to estimate some important parameters of the films. Such a study was complicated by the fact that the composition of the samples was inhomogeneous. At the same time, the demand for such a study is due to the need for the systematization of some previously formulated hypotheses and assumptions. Specifically, in the study concerned with analysis of the possibility of controlling secondary-ion emission from CdS–PbS films upon additional excitation with light with different spectra [6], some preliminary discussion is given regarding the fact that, in a complex heterophase semiconductor film, photoluminescence is defined not only by the concentration of emission centers, but by the distribution of these centers among the phases and by the structural distribution of the phases themselves within the film bulk as well. The urgency of studies of the mechanism of recombination in CdS–PbS films is evident when solving such applied problems as a reduction in charging of the films upon irradiation with charged particles and assessment of the locally concentrated energy.

2. EXPERIMENTAL

For the study, we used CdS(90%)–PbS(10%) photoconductive films. The films were about 1 μm in thickness and produced by vacuum sublimation onto glassy substrates coated by Al film electrodes in the form of interdigitated combs. The spacing between neighboring electrodes of the comb was ~120 μm; the length of each electrode was ~6 mm; and the electrodes had a Π-like shape. The deposition of a semiconductor film with the above-indicated composition over the electrodes followed by annealing in air at a temperature of 500°C for 30 min completed the for-

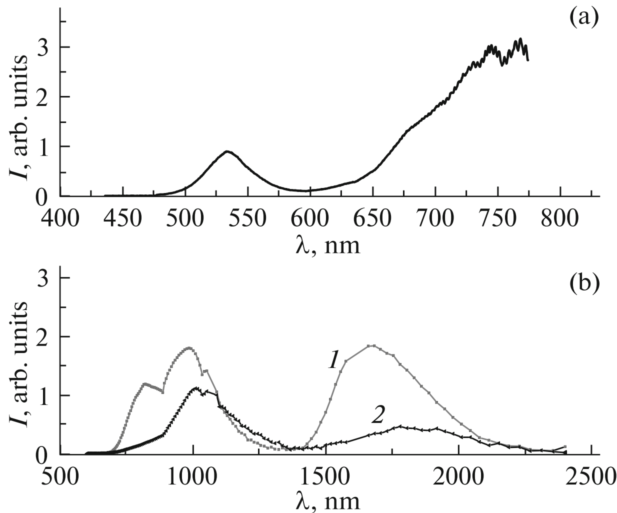

Fig. 1. PL spectra of a CdS–PbS film on a smooth glassy substrate. The spectra are excited by (a) 473- and (b) 532-nm laser radiation at the temperatures (*1*) 75 and (*2*) 300 K.

mation of a transverse photoresistor. To measure the photoconductivity in the longitudinal mode of the experiment, we used a clamping top electrode made from aluminum foil. The glassy-substrate side of the sample was illuminated with monochromatic light from an MDR-41 monochromator. The power at the output of the monochromator was determined with a calibrated FD-24K photodiode. Using the same monochromator, we studied the transmittance and reflectance spectra of the samples. From these spectra, we determined the absorption coefficient. To study photoluminescence (PL) in the visible and near-infrared (IR) spectral regions, we used a LabRam HR800 spectrometer combined with a confocal microscope (Jobin-Yvon Horiba) with a silicon detector. The spectrometer provided the possibility of using one of two excitation lasers emitting at the wavelengths 473 and 532 nm. These wavelengths are in the region of high absorption of the film, which was necessary to provide a high generation density of photoexcited charge carriers. To record the PL signal in the mid-IR region, we used a homemade system with an InGaAs photodetector. The substrate side of the sample was illuminated, whereas the PL signal was detected on the film side. The system also allowed us to conduct PL studies upon cooling. To do this, we placed the sample into a cryostat. The PL method provides a means for studying the excitation and recombination of photoexcited charge carriers in a comparatively small volume defined by the cross section of the laser beam. At the same time, in photoconductivity measurements, the whole sample (or at least the interelectrode gap) is commonly illuminated.

Studies of secondary-electron emission, cathodoluminescence, and the electron-beam-induced current (EBIC) were carried out with a Mira II Tescan LMU scanning electron microscope (SEM). The time of exposure of one point (pixel) to the electron beam, Δt, was 5.4 μs, and the total scanning time of the frame, t, was about 9 s. To detect the cathodoluminescence signal, we used a panchromatic detector sensitive in the wavelength range 350–650 nm. In the EBIC studies, a thin gold layer transparent to the electron beam was deposited onto the film surface by plasma-chemical deposition to form a contact with a Schottky barrier [8]. The second (ohmic) contact was the aluminum comb electrode. A thin copper wire was connected to both contacts with indium solder.

3. RESULTS

3.1. Photoluminescence

Figure 1 shows the PL spectrum of the annealed CdS–PbS film. The PL signal in the visible spectral region was excited with 473-nm laser radiation (Fig. 1a), and the PL signal in the IR region with 532-nm laser radiation (Fig. 1b). In the region of 520 nm, we observe edge emission with a photon energy close to the band gap of CdS. Such emission is characteristic of CdS powders and single crystals as well [9]. Another emission peak is in the range 750–800 nm, and this peak can be related to luminescence of the wide-gap phase of the CdS –PbS film (Fig. 1a) [10]. The peak at the wavelengths 920–930 nm (Fig. 1b) can be attributed to the presence of CdS–PbS alloy, since the solubility of CdS in PbS reaches 30% [11]. The PL signal in the IR region was excited with 532-nm laser radiation in order to excite first the wide-gap phase (the alloy of PbS in CdS) and then, via the wide-gap phase, the phases with narrower band gaps.

The nonequilibrium electron lifetime τ_n defined by interband radiative recombination is inversely proportional to the concentration of these electrons Δn. In the calculations presented below, for definiteness, we use the band gap of the alloy of CdS in PbS such that this band gap energetically corresponds to the luminescence maximum at the wavelength 1000 nm, for which the absorption coefficient is known (Fig. 2). At this wavelength, the characteristic absorption coefficient is small, and consequently, the effect of surface recombination is less significant and the PL signal is high in intensity. Thus, the lifetime τ_n is determined as

$$\tau_n = \frac{n_i^2}{R}\frac{1}{\Delta n} = \frac{n_i}{\sqrt{gR}}. \qquad (1)$$

Here, g is the generation rate of charge carriers and n_i is the intrinsic concentration of charge carriers in the narrow-gap component of the alloy of CdS in PbS. The concentration n_i is calculated by the formula

$$n_i = (N_c N_v)^{1/2}\exp(-\Delta E_g/2kT), \qquad (2)$$

where N_v and N_c are the effective densities of states in the valence and conduction bands, respectively; ΔE_g is

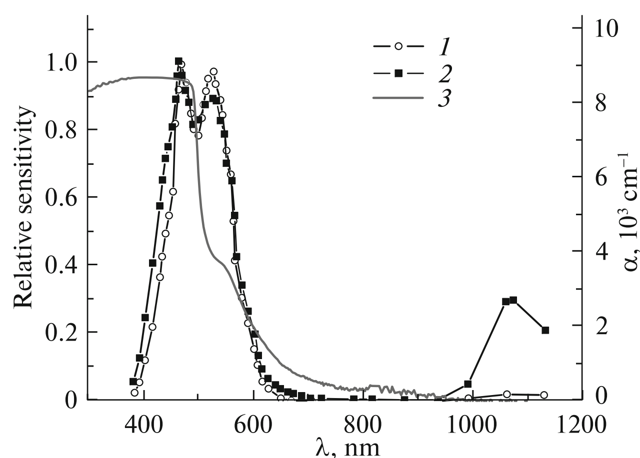

Fig. 2. Relative isoquant photosensitivity of a CdS–PbS sample in (*1*) the transverse and (*2*) longitudinal modes of measurements. Curve *3* refers to the absorption coefficient of the sample.

the band gap, T is temperature, and k is the Boltzmann constant. The number of photons emitted due to recombination, R, is described by the expression [12]

$$R = 1.785\times10^{22}(T/300)^4\int_0^\infty \frac{m^3\alpha u^3}{\exp(u)-1}du. \quad (3)$$

Here, m is the refractive index (approximately equal to the refractive index of CdS 2.5), α is the absorption coefficient, $h\nu$ is the photon energy, and $u = h\nu/kT$. In formula (3), the radiative recombination intensity during PL is theoretically calculated on the basis of general thermodynamic considerations, with invoking experimental data on absorption and without the involvement of data on recombination levels.

When cooled in air after annealing, the PbS phase (or, more exactly, the phase with the prevailing content of PbS) precipitates from the sublimated material in the form of separate crystallites. As shown previously [6], these crystallites are located at the sample surface. When the focused laser beam, whose diameter is comparable to the crystallite dimensions, is incident on the crystallites, the PL signal shifts to longer wavelengths corresponding to a higher content of PbS.

For example, the spatial resolution of the lens of the HR Horiba Jobin 800 setup was 360 nm for the wavelength 532 nm and 320 nm for the wavelength 473 nm. The laser beam was focused into a spot of a diameter of 1–2 μm at the sample surface. This diameter is comparable to the size of a large crystallite faceted as a trihedral prism (Fig. 3).

The IR luminescence bands with maxima at 1000 nm and in the range of 1600–2000 nm (Fig. 1b) are most likely defined by the recombination of charge carriers exactly in narrow-gap phases based on lead sulfide. Upon cooling, these maxima shift to shorter wavelengths, which is due to the positive temperature coefficient of the band gap of lead sulfide. Specifically, it is at such wavelengths that the PL maxima were observed in PbS (core)–CdS (shell) quantum dots (QDs) [13], in which the PL signal shifted to

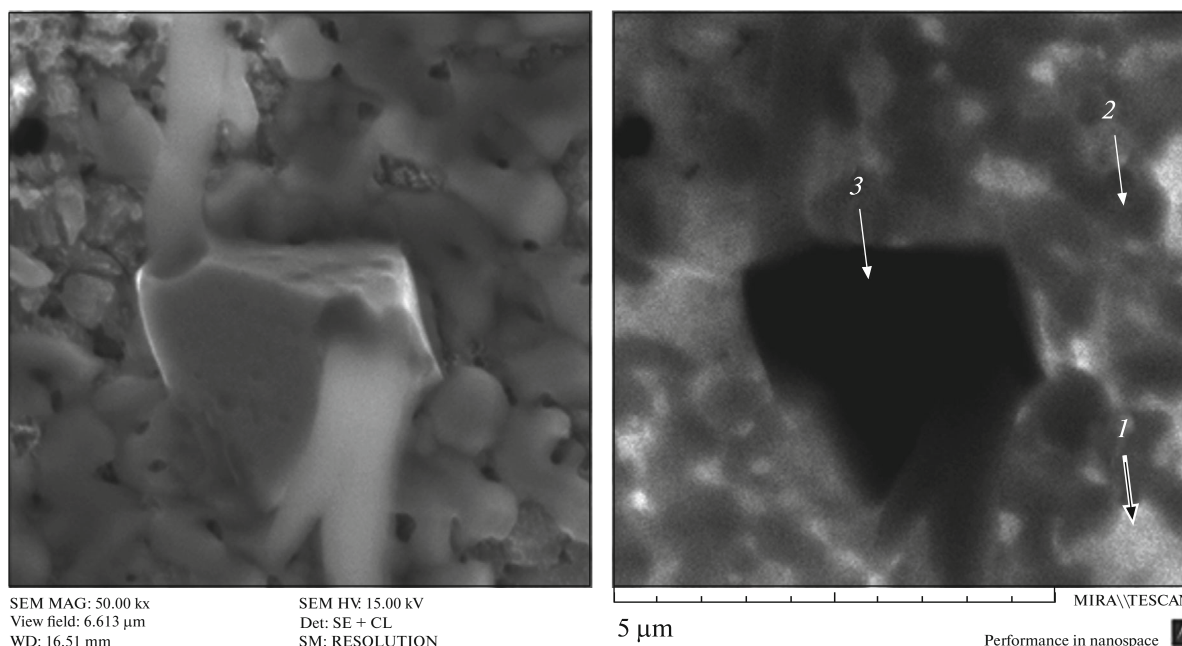

Fig. 3. Accumulation of (*2*, *3*) differently sized crystallites located over (*1*) the wide-gap phase. The images are obtained in (left) the secondary-electron and (right) cathodoluminescence modes of measurements.

Table 1. Energy positions of the photoconductivity and PL maxima (based on Figs. 1, 2)

Spectrum	Relative sensitivity maxima			PL maximums					
ΔE_g, eV	2.67	2.35	1.16	2.32	1.66	1.61	1.51	1.26	0.74

shorter wavelengths with respect to the PL signal from pure PbS due to a decrease in the QD dimensions.

Upon annealing in air, oxygen actively participates in the formation of cadmium and lead oxide phases. Therefore, oxygen can also participate in the formation of recombination drains. However, we previously showed that the manifestation of these drains and related effects (specifically, the lack of quenching of the "dark" conductivity because of a lack of residual conductivity) in cadmium-sulfide films was observed, only if lead sulfide was added to cadmium sulfide [14].

3.2. Photoconductivity

In considering the photoconductivity of films formed from limited CdS–PbS semiconductor alloys, we note that the films exhibit two regions of isoquant spectral sensitivity I_{ph}/N_ϕ, one in the visible spectral range 440–560 nm and the other in the near-IR range 1000–1200 nm, as shown in Fig. 2. Here, I_{ph} is the photocurrent and N_ϕ is the number of incident photons per unit time.

The visible spectral range is associated with the intrinsic photosensitivity of the CdS wide-gap phase and CdS-based alloys containing a rather small amount of PbS. In contrast, the photoconductivity in the near-IR region is defined by a larger fraction of PbS and a smaller fraction of CdS (the alloy that is closer to PbS in the phase diagram). The short-wavelength maximum at 460 nm should be mentioned separately. The origin of this maximum was not specially studied; it can be defined by the formation of lead oxide [15].

In the longitudinal mode of measurements, the amplitude of the long-wavelength maximum is higher. From our standpoint, this is due to the higher conductivity of the wide-gap phase because of the injection of majority charge carriers from the contact. Due to a decrease in the resistance of the wide-gap phase, narrow-gap inclusions gain the possibility of manifesting their spectral sensitivity which was previously limited by the series-connected wide-gap phase.

When comparing the energy of transitions corresponding to the PL and photoconductivity maxima (Table 1) with the band gaps of the crystalline phases, we can come to the conclusion that, in the region of the mutual solubility of components, there is a discrete set rather than a continuous series of alloys. By analogy with the theory of semiconductor lasers, in the interpretation, we here do not consider the role of recombination centers, since recombination centers themselves are thought to be more likely recombination regions rather than point defects [16]. It is worth noting that, in the samples similar to those under study, a high-intensity cathodoluminescence signal was previously observed in the IR region [2]. The steady-state photoconductivity is associated mainly with the wide-gap phase, and the narrow-gap phase manifests itself only in the longitudinal mode of measurements. In contrast, in PL measurements, the narrow-gap components manifest themselves more noticeably.

It is known that the photosensitivity spectrum can be substantially influenced by surface recombination. If incident radiation is absorbed irregularly through the sample thickness l and there is the diffusion of charge carriers, the photosensitivity of a quasi-monopolar n-type semiconductor (such as the CdS–PbS film under study) is described by the formula $I_{ph}/N_\phi = A(1 + S\alpha^{-1}/D_n)$, where $D_n = \mu_n kT/e$ is the diffusion coefficient of electrons, α is the absorption coefficient, μ_n is the electron mobility, A is a constant independent of the wavelength, and S is the surface recombination coefficient [17].

From the above formula, it follows that the dependence of I_{ph}/N_ϕ on α^{-1} in the region of the short-wavelength decrease in the photoconductivity ($\alpha l \gg 1$) is represented by a straight line, whose extension intersects the abscissa axis at the point $\alpha^{-1} = -D_n/S$ for any A, and the surface recombination rate S is determined from the slope of the straight line. For calculations by the above formula, we took the results partially reported in [18].

The surface recombination rate determined in this manner is 6×10^4 cm s^{-1} and is well reproducible from sample to sample. From comparison of the above value with the values of the surface recombination rate for CdS films produced by the same technology without PbS ($S = 6 \times 10^3$–10^4 cm s^{-1}) [19], we can see that the PbS addition makes the surface recombination rate several times higher. This result is attributed to the presence of an additional surface recombination channel responsible for the lack of residual conductivity in the CdS–PbS films [20].

3.3. Electron-Microscopy Studies

Figure 3 shows images obtained for the same region of an annealed CdS–PbS film in the electron backscattering and cathodoluminescence modes of measurements. Darker (*2*) and black (*3*) regions in the cathodoluminescence image correspond to the narrow-gap phase. These regions play the role of recom-

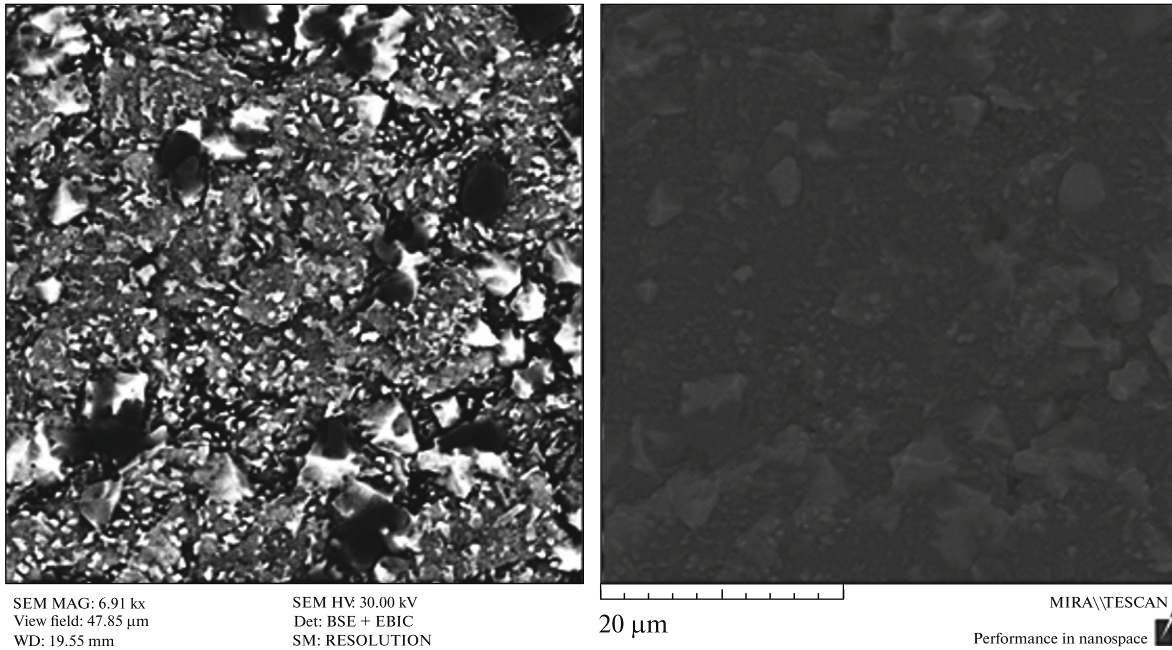

Fig. 4. Micrographs of a surface region of the annealed CdS(0.9)–PbS(0.1) film. The micrographs are recorded for the same region in (left) the electron backscattering and (right) EBIC modes of measurements.

bination drains, towards which excess nonequilibrium charge carriers move due to the concentration gradient [20] and in which high-intensity luminescence takes place [21].

It should be noted that the spatial distribution of charge carriers in the film in the longitudinal mode of measurements, can be roughly judged by scanning the surface with an electron beam and by recording the corresponding external current (EBIC) [22]. The micrograph in the EBIC mode of measurements (Fig. 4) shows that the currents induced by the electron beam flow mainly through narrow-gap crystallites at the sample surface. A micrograph of such crystallites in the electron backscattering mode of measurements is shown in Fig. 4 (left).

The dependence of the penetration depth of primary electrons d on their energy E_p is described by the expression [23]

$$d \approx 10^{-5} E_p^{3/2}/\rho, \tag{4}$$

where the density of CdS ρ is 4.8 g cm^{-3}. The energy E_0 needed for the generation of one electron–hole pair is determined by the semiempirical formula

$$E_0 = \frac{14}{5} E_g + E^*. \tag{5}$$

Here, the term E^* is proportional to the integral number of optical phonons lost in this process (0.5 eV < E^* < 1.0 eV).

Knowing the energy E_0 and the spatial distribution of energy losses, we determine two values of the generation rate of electron–hole pairs, the instant rate in the pulse (6a) and the average rate over the time of scanning of the whole image (6b):

$$g = \frac{J}{e}\frac{E_p}{E_0}\frac{1}{d}, \tag{6a}$$

$$g = \frac{J}{e}\frac{E_p}{E_0}\frac{1}{d}\frac{\Delta t}{t}. \tag{6b}$$

Here, J is the current density in the electron beam, e is the elementary charge, and E_p/E_0 is the number of pairs generated by one incident electron. (For example, in the case of cathodoluminescence (Fig. 3), the current of the electron beam that directly interacts with the sample and needed for calculation of the current density J is 350 pA; the diameter of this beam is ~5 nm.)

The calculation by formula (4) shows that, in the cathodoluminescence measurements, the accelerating voltage 15 kV allows electrons to propagate through the entire film thickness. Analysis of the recombination processes responsible for cathodoluminescence is based to a large extent on consideration of the integrated cathodoluminescence quantum yield η which is calculated, with consideration for surface recombination, by the simplest formula [24]

$$\eta = 1 - \frac{l_-}{d}\frac{S/D_n}{S/D_n + l^{-1}}(1 - \exp(-d/l_-)). \tag{7}$$

Here, the quantity l_- corresponds to the length of diffusion–drift displacement in the decelerating built-in

Table 2. Recombination parameters of CdS–PbS films at different excitation levels

	Excitation from monochromator, $\lambda = 532$ nm	Laser excitation, $\lambda = 532$ nm	Electron-beam excitation (cathodoluminescence)
Generation rate of pairs g, cm^{-3} s^{-1}	$\sim 10^{16}$	$\sim 10^{22}$	$\sim 10^{29}$ per pulse $\sim 10^{23}$ on average
Lifetime of nonequilibrium charge carriers τ_n, s	$\sim 10^{-4}$	$\sim 10^{-6}$	$\sim 10^{-7}$

field in graded-gap semiconductors $E = -(1/e)\nabla E_g$ (∇ denotes the first derivative with respect to the coordinate). Let us assume that, in magnitude, the quantity η is close to the quantum yield which is known for CdS-based cathodoluminescent phosphors from publications and approximately corresponds to 10^{-1} [25]. According to the Einstein formula, the diffusion coefficient for electrons is $D_n = \mu_n kT/e$. If we take $\mu_n \sim 50$ cm^2 V^{-1} s^{-1}, the diffusion coefficient is $D_n \sim 1$ cm^2 s^{-1}, and the reduced surface recombination rate is $S/D_n \sim 6 \times 10^4$ cm^{-1}. In (7), the equality converts into the identity at $l_- \sim 0.0006$ cm. The minimum diffusion length of electrons L_n in a graded-gap semiconductor with a built-in field is approximately equal to l_-. The electron lifetime determined from such calculations is $\tau_n = L_n^2/D_n \sim 10^{-7}$ s.

4. DISCUSSION

Summarizing, we can note that, in this study, we actually consider three cases of the generation of nonequilibrium charge carriers: the comparatively low generation level in photoconductivity measurements, the higher generation level in PL measurements, and the highest generation level upon excitation with an electron beam (Table 2). The recombination intensities in these three cases are different as well, since the lifetime of nonequilibrium charge carriers at high excitation levels is inversely proportional to the concentration of these charge carriers (see formula (1)). Apart from a successive increase in the intensity of the generation of charge carriers, a decrease in the area of excitation of nonequilibrium charge carriers accompany the above-described energy actions on the sample. It should be noted that this makes it possible to produce a degenerate electron gas in the local region of the sample. It is known that cadmium-sulfide single crystals as such possess laser properties that manifest themselves, for example, in the formation of an inverse population ($\sim 10^{21}$ cm^{-3}) by an applied electric field [26] or due to optical nonlinearity upon exposure to high-power pulsed laser radiation at 532 nm [27]. Therefore, it is reasonable to perform a comparative analysis of the effects of exposure of a heterophase sample with a dominant content of CdS to high-intensity fluxes of electrons and photons. To determine the lifetime of nonequilibtium electrons and the related generation rate in the PL process, we here use formulas (1)–(3) and the technical data of the Horiba setup. To determine the generation rate of charge carriers upon electron-beam excitation, we use formulas (4)–(7); in this case, the lifetime of charge carriers was calculated with consideration for the diffusion–drift parameters and quantum yield of CdS-based cathodophosphors. As concerns the lifetime and generation intensity of charge carriers in the photoconductivity studies of the sample illuminated by light from the monochromator, these parameters are taken from [20]. The results of the consideration of recombination processes in CdS–PbS films at different excitation levels are given in Table 2.

From Table 2, it can be seen that, according to estimates, the lifetime of nonequilibrium charge carriers decreases, as the excitation intensity is increased. This result should be expected. The role of nonradiative recombination at the surface can be judged from parameter S which can reach 6×10^4 cm s^{-1}; in this case, the recombination of photoexcited charge carriers can manifest itself in "loosening" of the crystal lattice and in the increased emission of secondary ions (anomalous secondary-ion photoeffect) [28].

The role of lead sulfide added to cadmium-sulfide powder to be subjected to vacuum sublimation can be seen from Table 3, which not only summarizes the results of this study, but generalizes the previously obtained results as well. From Table 3, it follows that the addition of PbS to CdS not only simply improves the characteristics of the films (suppressed inertia manifested by a lack of residual conductivity [14, 20], increased resistance to radiation [3]), but brings about the appearance of new effects (two types of SIPE [5, 28], an increase in the surface recombination rate).

Table 3. Comparison of the recombination properties of sublimated CdS and CdS–PbS films

Properties of CdS films	Properties of CdS–PbS films
Residual conductivity	No residual conductivity
Low surface recombination rate	Increased surface recombination rate
Low resistance to radiation	High resistance to radiation
Normal (negative) SIPE for Cd ions	Normal and anomalous (positive) SIPE for Cd ions

5. CONCLUSIONS

Summarizing the above-presented experimental data and calculations, we can formulate the main results of the study.

(i) A number of broad peaks in the IR region are detected in the PL spectra, which is apparently indicative of a discrete set of alloys of cadmium sulfide in lead sulfide.

(ii) According to the photoconductivity spectral data, the surface recombination rate exceeds the rates obtained previously for pure CdS films produced by a similar technology. This result is consistent with the previous assumption that there exists an additional recombination channel responsible for the lack of residual conductivity [20].

(iii) In combination with the data of the cathodoluminescence and EBIC micrographs, the dependence of the lifetime on the excitation intensity makes it possible to determine the prevailing directions of the draining of excess nonequilibrium charge carriers and the places of their possible recombination. As anticipated previously, these places are associated with the narrow-gap phase.

The results of the study can be thought as presenting a simplified concept of the features of recombination in polycrystalline films formed from limited CdS—PbS alloys as multiphase systems.

ACKNOWLEDGMENTS

The study was supported by the Russian Foundation for Basic Research, project no. 16-07-00226.

REFERENCES

1. Z. I. Kir'yashkina and A. G. Rokakh, *Photoconductive Films of the CdS Type* (Sarat. Gos. Univ., Saratov, 1979), p. 192.
2. S. I. Zolotov, N. B. Trofimova, and A. E. Yunovich, Sov. Phys. Semicond. **18**, 393 (1984).
3. A. G. Rokakh, A. V. Kumakov, and N. V. Elagina, Sov. Phys. Semicond. **13**, 462 (1979).
4. A. G. Rokakh, S. V. Stetsyura, N. B. Trofimova, and N. V. Elagina, Inorg. Mater. **35**, 452 (1999).
5. A. G. Rokakh, S. V. Stetsyura, A. G. Zhukov, and A. A. Serdobintsev, Tech. Phys. Lett. **32**, 30 (2006).
6. A. G. Rokakh and M. D. Matasov, Phys. Express **1**, 57 (2011).
7. S. V. Stetsyura, I. V. Malyar, and S. B. Venig, *Technology and Application of Heterogeneous Structures Based on Cadmium Sulphides Selenides* (Sarat. Gos. Univ., Saratov, 2013) [in Russian].
8. G. J. Russell, M. J. Robertson, and J. Woods, Phys. Status Solidi A **57**, 253 (1980).
9. O. N. Kazankin, L. Ya. Markovskii, I. A. Mironov, F. M. Pskerman, and D. N. Petoshina, *Inorganic Luminophores* (Khimiya, Leningrad, 1975), p. 37 [in Russian].
10. A. G. Rokakh, M. I. Shishkin, and N. B. Trofimova, in *Proceedings of the 2nd Russian Conference on Interaction of Microwave, THz and Optic Radiation with Semiconductor Micro- and Nano-Structures, Saratov, Russia, 2015*, p. 26.
11. Ya. A. Ugai, O. B. Yatsenko, V. N. Semenov, and E. M. Averbakh, Izv. Akad. Nauk SSSR, Neorg. Mater. **9**, 2055 (1973).
12. W. van Roosbroeck and W. Shockley, Phys. Rev. **94**, 1558 (1954).
13. M. J. Panzer, V. Wood, S. M. Geyer, M. G. Bawendi, and V. Bulovic, J. Display Technol. **6** (3), 90 (2010).
14. A. G. Rokakh, M. I. Shishkin, S. B. Venig, and V. S. Atkin, in *Proceedings of the 2nd Russian Conference on Interaction of Microwave, THz and Optic Radiation with Semiconductor Micro- and Nano-Structures, Saratov, Russia, 2015*, p. 35.
15. V. A. Izvozchikov and O. A. Timofeev, *Photoconductive Lead Oxides in Electronics* (Energiya, Leningrad, 1979) [in Russian].
16. A. N. Gruzintsev, Extended Abstract of Doctoral Dissertation (Inst. Probl. Microelectron. Technol. RAS, Chernogolovka, 1997).
17. V. F. Kiselev, S. N. Kozlov, and A. V. Zoteev, *Principles of the Physics of Solid State Surface* (Mosk. Gos. Univ., Moscow, 1999), Chap. 2, p. 63 [in Russian].
18. A. G. Rokakh and M. I. Shishkin, in *Proceedings of the 24th International Conference and School on Photoelectronics and Night Vision Devices, Moscow, 2016*, p. 132.
19. N. B. Trofimova, Extended Abstract of Cand. Sci. Dissertation (Sarat. State Univ., Saratov, 1976).
20. A. G. Rokakh and M. I. Shishkin, Prikl. Fiz., No. 2, 37 (2017).
21. I. V. Malyar, M. D. Matasov, and S. V. Stetsyura, Tech. Phys. Lett. **38**, 750 (2012).
22. C. Donolato, in *Physical Properties and Applications, Proceedings of the International School of Materials Science and Technology, Erice, Italy, July 1—15, 1984*, Ed. by G. Harbeke (Springer, Berlin, Heidelberg, New York, Tokyo, 1985), p. 138.
23. J. I. Pankove, *Optical Processes in Semiconductors* (Prentice-Hall, Englewood Cliffs, NJ, 1971; Mir, Moscow, 1973), Chap. 11.
24. G. P. Peka, O. A. Tokalin, and N. K. Dryapiko, Sov. Phys. Semicond. **17**, 682 (1983).
25. O. N. Kazankin, L. Ya. Markovskii, I. A. Mironov, F. M. Pskerman, and D. N. Petoshina, *Inorganic Luminophores* (Khimiya, Leningrad, 1975), p. 179 [in Russian].
26. N. G. Basov, A. G. Molchanov, A. S. Nasibov, A. Z. Obidin, A. N. Pechenov, and Yu. M. Popov, JETP Lett. **19**, 336 (1974).
27. H. P. Li, C. H. Kam, Y. L. Lam, and W. Ji, Opt. Commun. **190**, 351 (2001).
28. A. G. Rokakh and M. D. Matasov, Semiconductors **44**, 98 (2010).

Translated by E. Smorgonskaya